



ELSEVIER

Contents lists available at ScienceDirect

Ultramicroscopy

journal homepage: www.elsevier.com/locate/ultramic

Twenty years after: How “Aberration correction in the STEM” truly placed a “A synchrotron in a Microscope”

Quentin M. Ramasse

SuperSTEM Laboratory, SciTech Daresbury Campus, Keckwick Lane, Daresbury WA4 4AD, United Kingdom.

ARTICLE INFO

Article history:

Received 31 October 2016

Revised 6 March 2017

Accepted 14 March 2017

Available online xxx

Keywords:

Scanning transmission electron microscopy

Electron energy loss spectroscopy

Aberration-correction

ABSTRACT

Nearly two decades have passed since the Electron Microscopy and Analysis Group (EMAG) Conference was held in Cambridge in 1997, during which two seminal lectures were delivered that would influence the future of the U.K. electron microscopy community. With “Aberration correction in the STEM”, O.L. Krivanek and co-workers ushered in the era of probe-corrected scanning transmission electron microscopy, a powerful technology that L.M. Brown urged the community at large to embrace, arguing that it would be akin to placing “A Synchrotron in a Microscope”. This contribution will provide a personal account of how three generations of instruments installed at the SuperSTEM Laboratory, the national facility established after L.M. Brown’s vision, have made these powerful statements come true.

© 2017 Elsevier B.V. All rights reserved.

1. Introduction

The publication of this Festschrift honoring Ondrej Krivanek’s work and achievements happily coincides with the twentieth anniversary of the 1997 Electron Microscopy and Analysis Group (EMAG) Conference, held that year in Cambridge. Among other very distinguished speakers, Prof. L.M. (Mick) Brown delivered a seminal plenary lecture, which would arguably shape the future of the electron microscopy community in the United Kingdom and also inseparably tie it to Ondrej’s own work. In “A Synchrotron in a Microscope”, Mick Brown argues that electron energy loss spectroscopy (EELS) in the dedicated scanning transmission electron microscope (STEM) can in many cases “already match the performance” of synchrotron beamlines, at a fraction of their cost. He therefore urges the U.K. community to establish a national facility for STEM that would deploy the then-emerging aberration-correction technology [1]. Like all great visions, Mick’s call to the U.K. community was rooted in a reassuring level of insight and certainty. Earlier that summer, the Cambridge-based project to build a C_s corrector for STEM had seen the prototype instrument reach an important milestone and demonstrate a modest improvement in the spatial resolution of the base microscope, a Vacuum Generators (VG) HB5 STEM. In addition, M. Haider and J. Zach had earlier obtained similar success with correctors for scanning electron microscopes (SEM) and conventional TEMs based in large parts on H. Rose’s designs [2–4]. Although according to the legend it had taken all of Ondrej’s charm during a “stimulating discussion in a cosy pub” [5] to convince Mick of the viability of undertak-

ing such a project in Cambridge, results being published in the very same conference proceedings showed that “Aberration correction in the STEM” was now a reality [6]. Mick Brown could thus insightfully predict that it was soon to take the world by storm and the SuperSTEM Laboratory was established shortly thereafter to make his vision come true. Nearly twenty years later, as the U.K.’s National Facility for Aberration-Corrected STEM, the facility operates three generations of aberration-corrected instruments designed and supplied by Nion Company (or Colibris Company, as it was initially called for a very brief time), established by Ondrej Krivanek and Niklas Dellby following their departure from Cambridge. The first of these, a VG HB501 originally housed in Cambridge but retrofitted with a Nion Mark II quadrupole-octupole (QO) C_s corrector (see Section 3), could in a way be seen as the direct heir to that corrected VG HB5 prototype described in the EMAG 1997 conference proceedings.

“A Synchrotron in a Microscope” – how prescient and insightful have these words proved to be. The latest SuperSTEM instrument, a monochromated Nion UltraSTEM100MC ‘HERMES’ delivered in early 2015, not only incorporates an advanced Mark IV C_s probe corrector, but also a high-energy-resolution monochromator, which enables spectroscopy experiments in the sub-10meV energy resolution regime [7]. This instrument now arguably surpasses the capabilities of synchrotron beamlines, in some specific cases at least.

Twenty years on, these pages provide a rather personal account of the impact these two EMAG proceedings papers, “A Synchrotron in a Microscope” and “Aberration correction in the STEM”, have had on a generation of microscopists ‘growing up’ in the aberration-corrected era that was ushered in by the EMAG 1997 conference, and briefly detail the successive generations of Nion

E-mail address: qmrmasse@superstem.org

<http://dx.doi.org/10.1016/j.ultramic.2017.03.016>

0304-3991/© 2017 Elsevier B.V. All rights reserved.

Please cite this article as: Q.M. Ramasse, Twenty years after: How “Aberration correction in the STEM” truly placed a “A synchrotron in a Microscope”, Ultramicroscopy (2017), <http://dx.doi.org/10.1016/j.ultramic.2017.03.016>

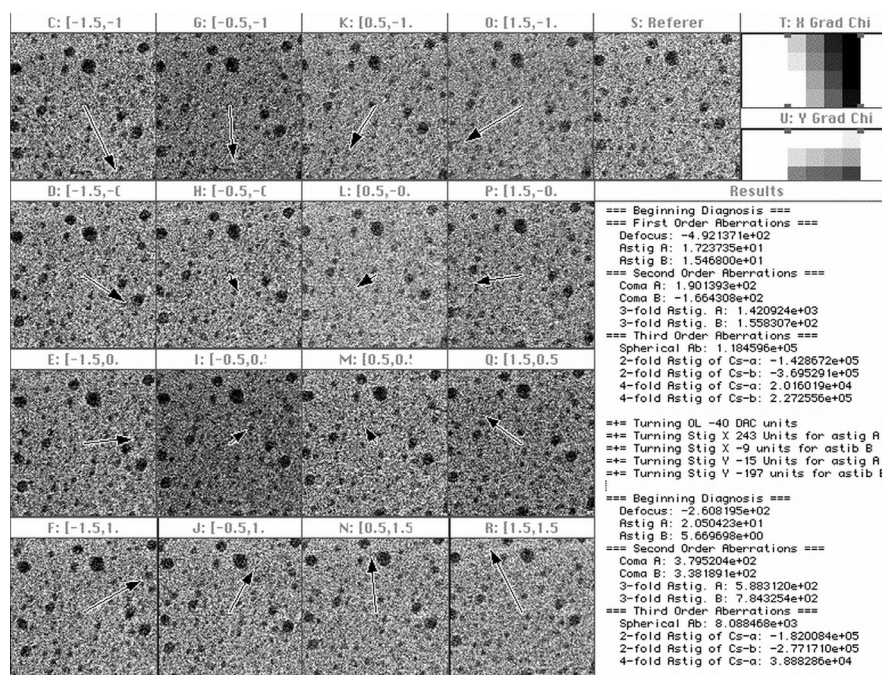


Fig. 1. Original tuning window for the prototype C_s corrector software. The algorithm is based on assessing tilt-induced shifts of features in scanned bright field images and closely related (by reciprocity) to the auto-tuning method described by Krivanek et al. [14]. Reproduced from [15].

microscopes. This article also aims at revisiting and honoring Mick Brown's and Ondrej Krivanek's vision through recent results from the latest SuperSTEM microscope, which already show hints that their predictions from 1997 have not only become reality but have by and large been surpassed beyond what anybody attending these EMAG lectures would have imagined – save perhaps for the main protagonists themselves.

2. Aberration diagnosis

It is generally accepted that the lack of fast and automated aberration diagnosis methods (or auto-tuning) was one of the main factors that prevented for nearly fifty years the successful implementation of aberration correction in the TEM (for a review and discussion of other factors, see e.g. [8] and references therein). Famously, this is in spite of the general principles having been outlined by O. Scherzer as early as 1947 [9]. The strong emphasis placed by Krivanek et al. on the role of software designed to measure and adjust the aberrations in early reports of the working STEM QO correctors is striking [6,10,11]. Without them, “one is faced with a fuzzy image, a large number of controls and no useful procedure for making the image sharper” [6]. The drive towards automation is best exemplified through Ondrej Krivanek's own earlier contributions to the field of aberration measurement, long before the inception of the Cambridge QO C_s correction project. Single diffractogram analysis to determine defocus and C_s [12], or repeated (no doubt hurried!) trips from the microscope room to the optical bench *via* the dark room in order to analyse diffractograms and stigmatize a high voltage instrument [13], eventually led to some level of automation thanks to the advent of charge-coupled devices (CCDs) [14]. The original tuning algorithm for the Nion prototype corrector described in the EMAG1997 conference proceedings is closely related through reciprocity to the procedure described in the latter, using tilt-induced shifts (TIS) in a series of scanned bright field images to derive the aberration function, as illustrated on Fig. 1 [14,15].

Attempts to devise faster, more precise, more universal diagnosis tools for STEM to replace the original TIS method provided

the basis for at least two generations of doctoral students at the Cavendish Laboratory in Cambridge [16,17] but also elsewhere [18], continuing the effort that had been initiated as part of the C_s corrector development project. Reviewing the many contributions to the field would no doubt be beyond the scope of this article and interested readers are encouraged to consult A.R. Lupini's masterful treatment of many aspects of aberration measurement [19], including his own contribution based on the analysis of a series of Ronchigrams. The realisation that the Ronchigrams' local magnification could be linked directly to the second derivative, or Hessian, of the aberration function [20,21] is still to this day at the heart of the tuning algorithms employed on Nion microscopes [22]. Interestingly, and despite successful attempts to devise techniques that can be applied to crystalline materials [19,23], most algorithms deployed in aberration-corrected STEMs today still suffer from a lack of universality. They often require a very specific object type to converge satisfactorily, either some amorphous area of the sample potentially far away from the region of interest, or a dedicated tuning sample altogether [18]. It is perhaps a testament to the stability of modern correctors that the implementation of universal tuning algorithms has not been pursued more actively, the existing solutions clearly providing enough usability for most applications. The ‘achromatic line’ approach of Ramasse et al. [23] for measuring non-round aberrations from on-axis crystals for instance, although fully functional and tested on SuperSTEM instruments, was never practical or fast enough to supplant (or indeed complement) the main Ronchigram-based autotuning routine: Fig. 2.

It is nevertheless an essential aspect of aberration correction inherited from the push for implementation in the late 1990s which is still a very active field of research. As corrector technology progresses the precision measurement requirements become more stringent. More advanced, faster algorithms are therefore needed [24,25]. The ability to implement such algorithms online to provide dynamic diagnosis and correction has also seen a renewed emphasis in an effort to ensure long-term time windows of corrected state for increasingly complex optical instruments [26]. The use of fast pixelated cameras as ‘universal STEM detectors’, which promises to become increasingly wide-spread [27,28],

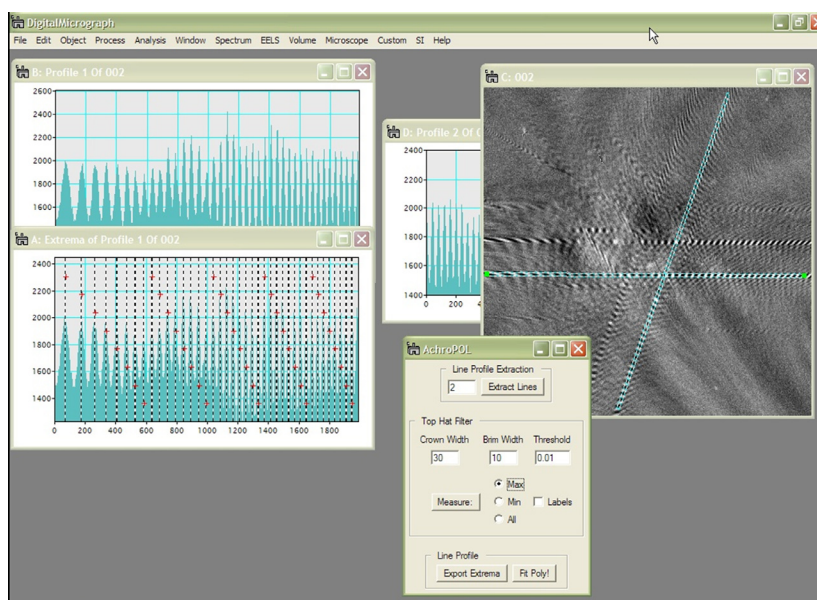


Fig. 2. Screenshot of the implementation in the Digital Micrograph software suite of the ‘achromat line’ tuning algorithm of Ramasse et al., which uses Ronchigrams averaged through focus (rightmost window) to measure non-round aberrations from on-axis crystalline samples. Although accurate, it was never practical enough to be systematically used alongside the otherwise convenient and reliable main auto-tuning routine [23].

is likely to rekindle interest in this topic thanks to the ability to record enough information to both generate images and measure aberrations at the same time [29].

3. Nion mark II correctors: SuperSTEM 1 and the NCEM vG

Mick Brown’s “A Synchrotron in a Microscope” suggested that if “one tenth of the proposed cost of [the then-envisioned replacement U.K. synchrotron, to be called] Diamond and its beam lines could be invested in a national center for STEM, [...] with £15M capital, and a staff of 30, one could imagine commissioning an array of specialised instruments including dedicated STEM with a performance far superior to any existing instrument” [1]. It is interesting in hindsight to also read the suggestion to site the proposed centre for STEM at the Central Laboratory of the Research Councils in Daresbury “to capitalise on the resources already deployed there”. This is indeed where the SuperSTEM laboratory would eventually be founded (more on this below), but the suggestion also reprises a widespread concept, whereby large scale facilities and National Laboratories with synchrotron radiation sources are also hosts to advanced user facilities for electron microscopy (Lawrence Berkeley National Laboratory, Brookhaven National Laboratory, Argonne National Laboratory...). Although a synchrotron is in some cases already in the microscope (an intentionally-provocative and somewhat mischievous statement, of course), there are nevertheless obvious advantages in having both types of facilities together. The prospect of exploiting such synergies has clearly lost none of its appeal, as the establishment of the electron Physical Sciences Imaging Centre (eP-SIC), a new microscopy facility at the Diamond light source (which as it turns out was not built in Daresbury in the end but in Harwell instead, unlike the SuperSTEM Laboratory...) would seem to indicate. True synergistic studies making use of both a synchrotron and a microscope on the very same sample are rare however, due in no small part to the very different sample requirements for the two types of experiments. Although Mick Brown notes that “the time to prepare the sample and acquire the spectra is about the same for the two techniques”, in the STEM case a sample needs an “electron transparent edge, perhaps 50 nm thick”, while in synchrotron-based X-ray absorption spectroscopy, data is

obtained from “many hundred randomly-oriented grains” [1]. Recent studies using portable micro-reactors that can be mounted in both a synchrotron beam line and an electron microscope sample holder nevertheless demonstrate the strength of such a combined approach in the specific case of *operando* catalytic reactions where the sample is by design thicker [30].

Funding for a National Facility along the lines suggested in Mick Brown’s EMAG lecture was finally secured, and the SuperSTEM Laboratory was established in Daresbury, Cheshire, with Prof. Andrew Bleloch as its inaugural director (Prof. Peter Goodhew acting as the Principal Investigator for the project). The initial instrument, ‘SuperSTEM 1’ as it would become known, was once again one of the Cavendish Laboratory’s VG microscopes, a later generation HB501 100 kV instrument retrofitted in Cambridge with a Nion Mark II QO C_s corrector prior to its move North. Fig. 3 shows a picture taken during the retrofit in the summer of 2002, a process overseen by the corrector designer and Nion President, Ondrej Krivanek himself (for the second time only, after the installation of the IBM TJ Watson Research Centre instrument [31], apparently also one of the last [5]).

Although a very early adopter of the technology and indeed the very first laboratory in the U.K. to offer open user access to an aberration-corrected instrument, SuperSTEM was by no means alone (nor the first) in embarking on a “road that should ultimately lead to an era of lab-sized STEM instruments able to routinely achieve 1 Å or even 0.5 Å resolution” [6]. Other VG microscopes were being fitted with correctors, the first of which was installed at IBM TJ Watson Research Centre where Batson et al. demonstrated for the first time the formation of probes smaller than 1 Å on a VG HB501 operated at 120 kV [31]; or at Oak Ridge National Laboratory where Nellist et al. were able to demonstrate 0.78 Å spacing in silicon using a Nion corrected VG HB603 operating at 300 kV [32]. During the same period, other microscope manufacturers were also successfully incorporating probe correctors, such as those designed by CEOS, in their instruments [33,34]. One should hasten to point out that although the resolution race was probably never an end in itself, the excitement of “going sub-Å” was undeniable. The micrograph in Fig. 4a shows a high angle annular dark field (HAADF) image of GaN in [0001] orientation

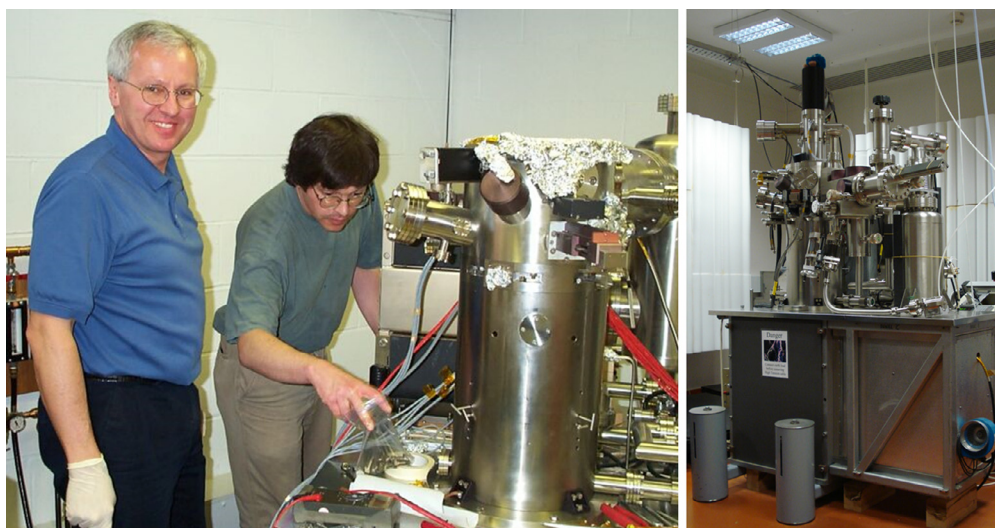


Fig. 3. Ondrej Krivanek and Andrew Bleloch during the installation of the Mark II Nion corrector into the then-called 'SP501' VG HB501 microscope, which would become the SuperSTEM 1 instrument (right, after its installation in Daresbury). Photograph courtesy of Dr. U. Falke.

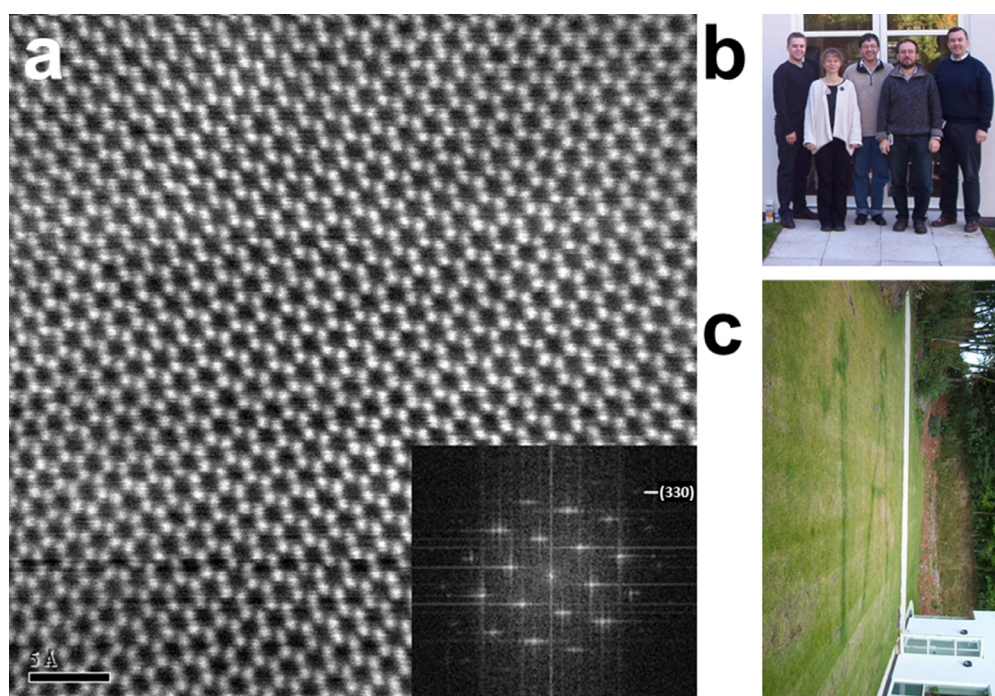


Fig. 4. *a)* HAADF image of [0001] GaN acquired on SuperSTEM 1. The Fourier transform, at the bottom right, shows information transfer beyond the 1 Å level. *b)* The original SuperSTEM crew: (left to right) Will Costello, Meiken Falke, Andrew Bleloch, Uwe Falke and Peter Shiels. *c)* Celebratory sub-Å lawn graffiti in front of the SuperSTEM building.

whose Fourier transform, inset, reveals transfer up to the (330) diffraction spots, acquired *ca.* spring 2004. The SuperSTEM crew celebrated reaching this milestone themselves with some inventive lawn graffiti: Fig. 4c.

The associated project which brought this particular sample to SuperSTEM was a collaboration with scientists from Lawrence Berkeley National Laboratory. It had been concerned with investigating the atomic and electronic structure of dislocations, imaging and probing with EELS for the first time the complex atomic arrangements of mixed dislocations in GaN [35]. More in-depth reviews of the wide range of materials science investigations that was enabled by the provision of a user centre for aberration correction can be found elsewhere [36], including the description of early successes in elucidating the peculiar atomic structure of a

2×1 reconstructed $\text{NiSi}_2/\text{Si}(001)$ interface, which had only just been predicted by theory but hitherto never observed [37]. This was a clear demonstration of the power of “directly interpretable” aberration-corrected HAADF imaging of defects and interfaces and a poster child result for SuperSTEM: Fig. 5.

The GaN results have a particular significance, however. On the one hand, this work demonstrated that it was possible to probe with EELS the electronic structure of complicated defects such as dislocations, atomic column by atomic column, without recourse to the “difference method” advocated by Brown in “A Synchrotron in a Microscope”. It should nevertheless be pointed out that such experiments are still far from routine today. Complex inelastic signal simulations (made even more so by the fact that the structure of interest is defected) are necessary to rationalise and interpret the

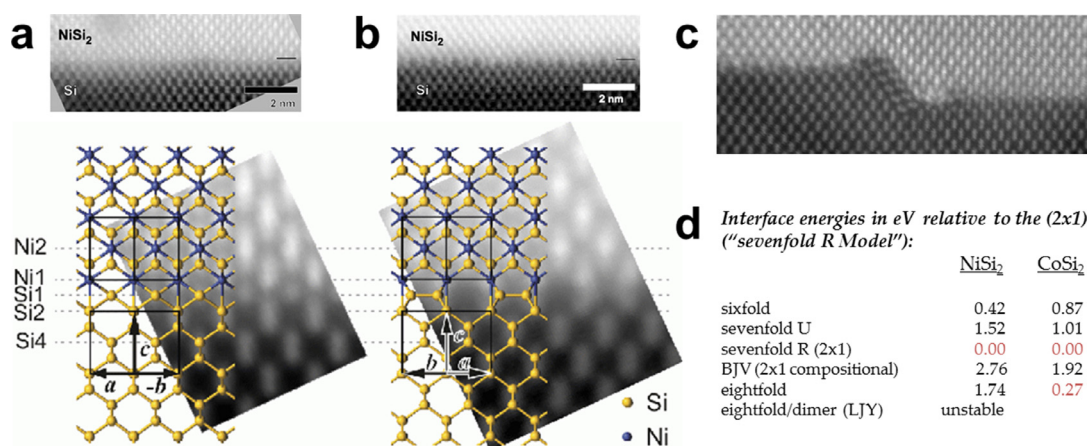


Fig. 5. *a-b)* HAADF images of the two variants of the NiSi₂/Si(001) interface, with overlaid ball-and-stick model. *c)* HAADF image of the interface showing a complex defected transition from a reconstructed section (left) to a non-reconstructed section (right). *d)* calculated energies for various interface structures – the lowest energy models are those most commonly found in HAADF images. Adapted with permission from Falke et al. [37], copyrighted by the American Physical Society.

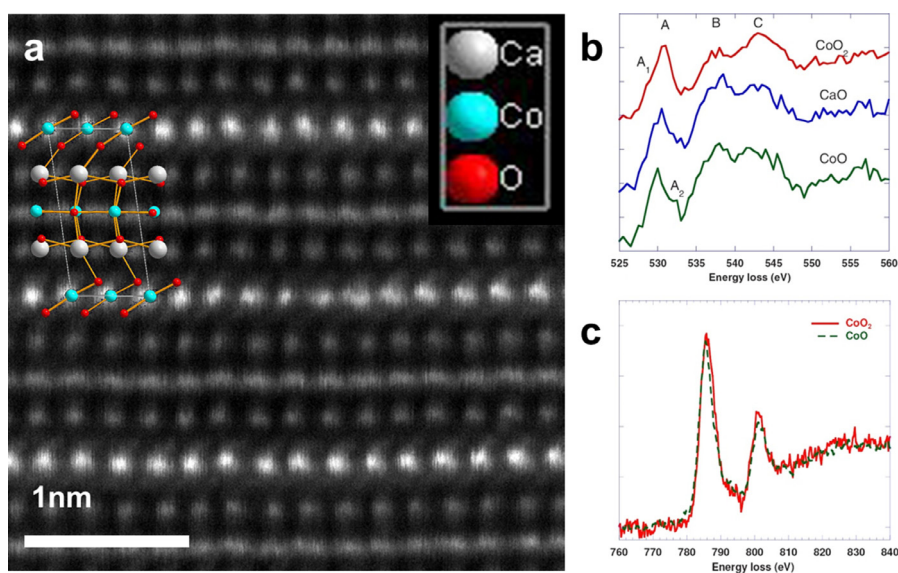


Fig. 6. *a)* HAADF image obtained on the TEAM 0.5 microscope at NCEM at 300 kV showing the incommensurately-stacked structure of thermoelectric oxide Ca₃Co₄O₉ in [010] projection. Faint contrast on either side of the Co columns in the CoO₂ layer suggests that O columns are being imaged. The Co columns in the Ca₂CoO₃ rock-salt layers are less resolved, suggesting the presence of structural modulations through the sample thickness. *b-c)* Layer-resolved EELS (O K edge and Co L_{2,3} edge) acquired on the NCEM VG showing differences between probe positions, indicative of charge transfer between layers. Adapted with permission from Yang et al. [41], copyrighted by the American Physical Society.

experimental data [38,39]. On the other hand, one of the collaborators on the project (Prof. N.D. Browning) was soon to purchase another Nion-corrected VG HB501, the first aberration-corrected instrument at the National Center for Electron Microscopy (NCEM) in Berkeley, USA, which would provide NCEM an introduction to the wonders and complexities of the aberration-corrected world in anticipation of the arrival of the TEAM microscopes [40]. Perhaps because of the greater familiarity with VG microscopes of the main operator of that instrument, the NCEM VG served for years as the analytical microscope of choice to generate EELS data complementary to the world-leading imaging abilities of the TEAM 0.5 microscope [39,41,42]. Fig. 6 shows for instance how spatially-resolved differences in EELS signature, indicative of charge transfer between layers of a Ca₃Co₄O₉ misfit thermoelectric oxide, are probed on the NCEM VG, while the crystal structure is imaged with great clarity on the TEAM 0.5 microscope, revealing structural modulations in the Co columns of the rock-salt sub-system. A winning team, no doubt.

It is this combination of imaging and EELS in the STEM at atomic resolution that arguably has had the largest impact on materials science, a theme central to Brown's and Krivanek's thesis, as they foresee in 1997 instruments able "to deliver probe currents into atom-sized regions that are large enough for rapid and sensitive EELS and EDXS analysis" [6]. Indeed, going further than point-by-point EELS analysis, SuperSTEM 1, along with other instruments of the same generation, were soon producing the first two-dimensional inelastic images of crystals [43,44]. Two-dimensional EELS (and EDXS) mapping has now become almost routine, taken to new heights and scales thanks to the increased stability of a new generation of corrected instruments and to performance improvements in spectrometers [45]. But it is perhaps from a less foreseeable source that the crowning achievement of the Mark II correctors would come, as Mhairi Gass, Ursel Bangert and their team used SuperSTEM 1 to image directly at (near-)atomic resolution that most exotic of crystals, single-layer graphene. In the same set of experiments they also provided the EELS spectroscopic fingerprint of the stacking sequence of graphene layers through

spatially-resolved plasmon-region peak variations [46]. Interestingly, while discussing this and other papers on graphene appearing roughly at the time, Ondrej did presciently remark that “he would not be surprised if Andre Geim were awarded the Nobel Prize sooner rather than later”, paraphrasing [47]. The rest, as they say, is history... This pioneering work would nevertheless also make SuperSTEM 1's limitations quite clear: even when imaging graphene at 100 kV the atoms were not perfectly resolved, and the need for lower voltages to avoid damaging these one-atom-thick carbon layers meant that spatial resolution would suffer. A new type of synchrotron-in-a-microscope was needed, one that would provide enough flexibility in operational parameters to mitigate beam damage by lowering the beam energy with a minimal spatial resolution penalty.

4. UltraSTEM – the “gentle STEM” era

The term “gentle STEM” was coined by Ondrej to denote the combination of a low acceleration voltage (typically 60 kV) and clean column vacuum [48,49]. This approach is of course only ‘gentle’ to a certain category of objects, which mostly suffer from knock-on damage from the more energetic (100 kV or over) electron beam rather than from ionisation, the latter having a tendency to become more severe as the beam primary energy is lowered [50]. This flavour of ‘gentle’ STEM is thus poorly suited to the vast majority of organic samples and other approaches must be deployed for different types of beam-sensitive materials. Nevertheless, ‘gentle’ low-kV STEM, and from a Nion user's perspective its implementation in Nion's third generation instrument, the UltraSTEM, ushered in the era of ‘single atom microscopy’. The first model of these was delivered to the SuperSTEM facility in 2006 where it became known as SuperSTEM 2. Technically, it should be said that it was in fact the second UltraSTEM column built at the factory, but administrative issues had made it essential that it be delivered ahead of its slightly older sibling, due to be sent to Cornell University.

The tremendous stability of (clean) graphene under the electron beam in gentle STEM conditions made it, and to an extent other 2-dimensional materials such as hexagonal BN and transition-metal dichalcogenides such as MoS₂, the perfect sandbox to apply the imaging and spectroscopy abilities of the new Nion UltraSTEM100 microscope. By maintaining a probe size close to 1 Å in spite of the acceleration voltage being lowered to 60 kV, below the knock-on threshold of the atoms in the sample, the UltraSTEM made it possible to image and identify unambiguously every single atom. This ability was put to great use, from ground-breaking images of single-layer h-BN obtained on the ORNL UltraSTEM [51], to the observation of unique structure reconstructions at the edge of MoS₂ nano-catalysts [52] or the demonstration of the propensity of graphene to spontaneously ‘heal’ itself when perforated [53]; Fig. 7. Again, one must emphasise the extreme specificity of the type of samples used in these studies: 2D materials are ideal systems for this approach to quantitative imaging precisely because they are only one (or at a stretch, a few) atom(s) thick.

Single-atom impurities or defects in 2D materials can also be chemically fingerprinted using spectroscopy. Among many exciting results, this approach led to the unambiguous identification in EELS of heavy atoms with very similar atomic numbers (La and Ce) captured in carbon nano-peapods, where the interpretation of Z contrast alone may have been difficult [54] or to the verification of the implantation levels of N or B ions within single-layer graphene [55]. It even provided the first demonstrations of single atom detection with photons [56,57]: Fig. 8. Lovejoy et al. argue that the ability to record simultaneously and quantitatively EELS and EDXS from a single atom provides the opportunity to compare the experimental intensities to standard-less estimates, thus exploring the

validity of tabulated inelastic cross-sections [56]. At a time when microscopy is becoming increasingly more quantitative and with many research groups attempting to provide true metrology at the single atom level through both imaging and spectroscopy, it would seem a worthwhile, albeit very time-consuming, project to explore this suggestion further and attempt to systematically compare theory and experiment.

It is perhaps also interesting to shortly comment on the experimental requirements for this type of experiments. With the instrumentation really at its ultimate detection limit, detectors optimised specifically for low voltages can make the detection of single atoms more efficient [57]. But arguably they also risk making the microscope less versatile, departing from that idea of an instrument as suited as a synchrotron to a very wide variety of materials science questions. In a very convincing argument for dedicated, specialised instruments, Ondrej often makes a motoring comparison, suggesting it would be akin to asking the owner of a Ferrari to use it for the school run or to tow the family's caravan to the coast for the holidays. In the context of a user facility such as SuperSTEM, and likely at many other laboratories, it is perhaps also important to keep in mind the need to find a suitable balance between specificity, performance and versatility, lest the Ferrari should only be delivered with a gear box stuck in the highest gear.

Having shown what atomic species are present and where they are located, some fundamental questions remain: how exactly are these atoms bonded to one another and how do structural differences affect their electronic configuration? Studying the fine structure of electron energy loss spectra can provide answers to these questions, thanks to synchrotron-level energy resolution obtained at the single atom level through the near-Å size of the electron probe. Aside from the ‘UltraSTEM community’, Kazutomo Suenaga and his team at AIST in Tsukuba, Japan, showed, using altogether different although certainly no less capable microscopes, how the EELS fine structure of single carbon atoms at the edge of graphene (or of N atoms at defects in single-layer hexagonal BN) differed depending on their coordination [58,59]. Similarly, both the ORNL and the SuperSTEM groups independently showed how 4-fold coordinated and 3-fold coordinated Si substitutional impurities in graphene possess dramatically different Si L edge fine structures [60,61]. It is the striking agreement with spectra calculated *ab initio* using density functional theory (DFT) that makes these results all the more remarkable. The case of the 3-fold coordinated Si is particularly instructive: relaxing the structure in three dimensions shows that the Si atom's lower energy configuration is slightly out of the lattice plane (as it prefers to adopt a near-sp³ configuration, as would be the case e.g. in SiC). However, the energy difference with a structure obtained by enforcing a fully planar geometry is minimal. The calculated EEL spectra for the two models differ drastically, however. The three-dimensional out-of-plane model leads to a near-perfect match to experimental data while the match is far less convincing otherwise in the planar case: Fig. 9. This combination of experiment and theory can thus distinguish between two models of a material that differ by three-dimensional structural distortions of a mere few pm. Conversely, obtaining such a perfect match between experiment and theory provides a very strong validation of the calculated model, which can in turn be interrogated for other physical properties not easily or directly accessible from the experimental EELS data. This was the approach taken by Kepaptsoglou et al. in demonstrating the presence of direct EELS fingerprints for the p-type and n-type doping of graphene through the introduction *via* ion implantation of substitutional B and N impurities [62]. With STEM-EELS and DFT opening the door to physical chemistry at the single atom level, had this generation of instruments then finally realised the ultimate “Synchrotron in a Microscope”?

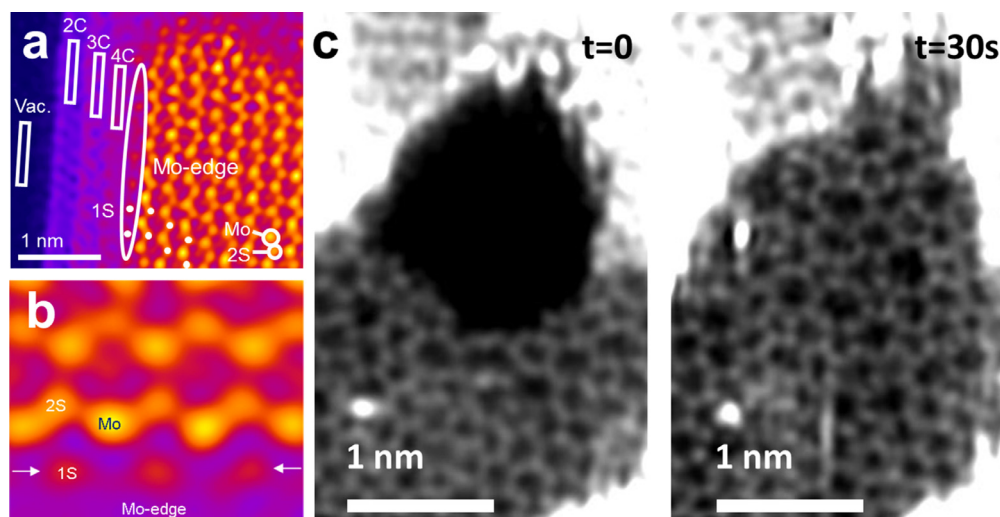


Fig. 7. *a-b*) HAADF images (processed with a maximum entropy probe deconvolution algorithm) of single-layer MoS₂ nano-catalysts on a thin graphite support, acquired on SuperSTEM 2 at 60 kV acceleration voltage. Careful analysis of the image intensity allows unambiguous element identification and reveals that the Mo edge of the particle is terminated by a single S atom. Adapted with permission from Hansen et al. [52], copyrighted by John Wiley and Sons. *c*) HAADF images (processed with a maximum entropy probe deconvolution algorithm) of a hole in single-layer graphene filling up with a near-amorphous 2-dimensional structure [53].

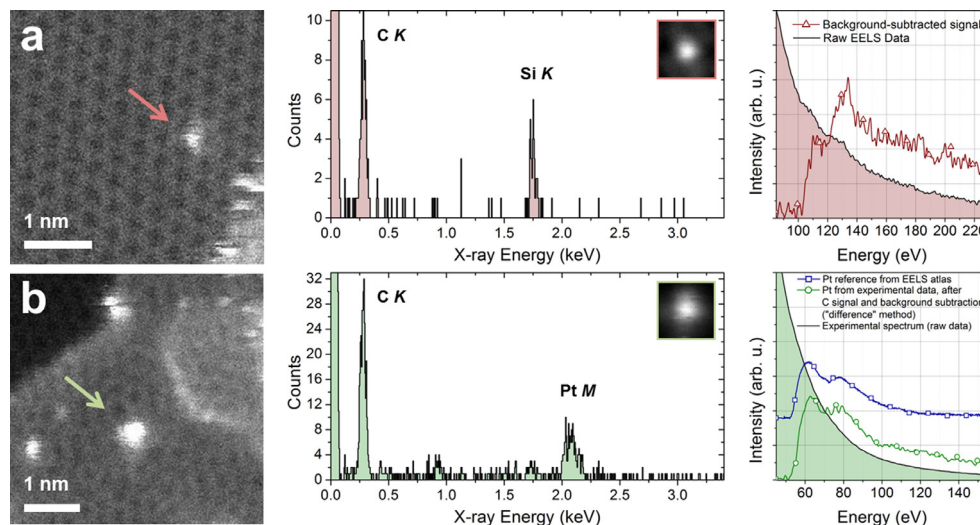


Fig. 8. *a*) HAADF image of a single substitutional Si atom in single-layer graphene, along with the EDX spectrum acquired by scanning the beam repeatedly over the small area pictured as inset, recentering the subscan window over the Si atom. An EELS spectrum is acquired simultaneously with the EDX spectrum. *b*) HAADF image of a single Pt impurity atom sitting on top of carbon base contamination covering the single layer graphene sheet, along with the EDX spectrum acquired by scanning the beam repeatedly over the small area pictured as inset, recentering the subscan window over the Si atom. The EELS spectrum acquired simultaneously with the EDX spectrum requires intensive data processing (here using the ‘difference method’) and comparison with reference data to identify the Pt edges. [56].

5. HERMES: the synchrotron in a microscope

A number of paragraphs in the EMAG proceedings paper have so far been conveniently ignored in this article. While the typical synchrotron-based X-ray absorption spectroscopy (XAS) beamlines with “energy resolutions of 0.25eV” are “already matched by the dedicated STEM”, Brown concedes that “some [beamlines] are designed to achieve very high energy resolutions (20meV) and small spot sizes (10 μ m or so)”. Even without reaching the 20meV level, improvements over the cold field emitter’s native energy width of approximately 0.30 eV were needed to help addressing some of the topics listed by Mick Brown in the paper: observation of excitons, observation of band gaps.

The recent commissioning of a third generation of SuperSTEM instrument (and generally the development of advanced high-energy-resolution monochromators: a similar project is *e.g.* also under way in Japan in collaboration with JEOL Co. [63]) has now

undoubtedly bridged that gap. Aptly named ‘SuperSTEM 3’, the monochromated Nion UltraSTEM100MC ‘HERMES’, the third of its kind at the time of writing after early deliveries to Rutgers and Arizona State Universities, already reaches routine sub-20meV energy resolution. It promises to enable a range of new and unique experiments hitherto impossible on any other type of electron microscope: Fig. 10. As with the initial two SuperSTEM instruments, its funding was secured as a result of a consultation of the U.K. electron microscopy community, with the clear goal to make it a shared facility and to provide early widespread access to this truly record-breaking technology. Mick Brown’s call for “the community of electron microscopists, working together, so that a unified project can be presented to the Research Councils” has not faltered, and only a year after commissioning the new microscope the response and appetite of the scientific community for this new capability has been exceptional. The prospect of carrying out ‘Raman-

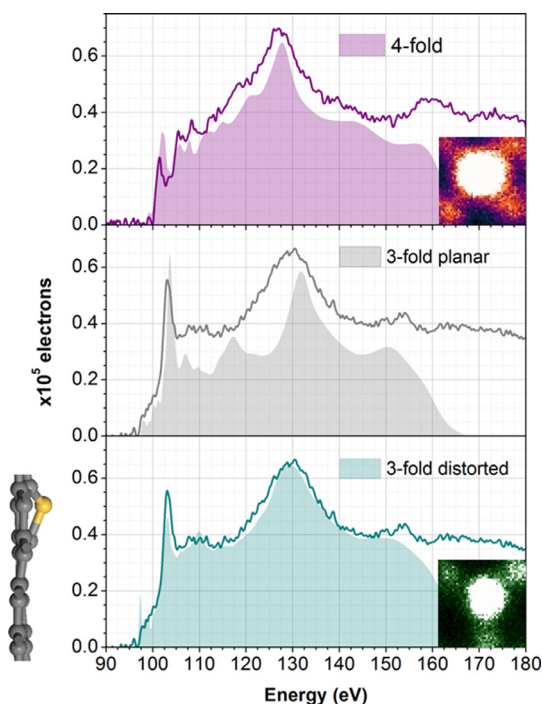


Fig. 9. Comparison between experimental spectra (solid lines) after background subtraction using a decaying power law, and the spectra calculated by DFT (shaded areas) for a 3-fold coordinated Si substitutional impurity in graphene and a 4-fold coordinated Si. Experimental spectra were acquired by scanning repeatedly a small area centred around the Si impurity and accumulating 1 s EELS exposures. 50 frames of the simultaneously-acquired HAADF movie are averaged to generate the image of the Si and its C neighbours, inset. Relaxed models of tetravalent and trivalent Si atoms within a single-layer graphene sheet were created to calculate the theoretical spectra with CASTEP: the atomic positions were optimised using DFT calculations. In the '3-fold distorted' case, the Si atom was allowed to relax out-of-plane: bottom model.

like' vibrational spectroscopy in the STEM, with a nm-sized probe or smaller is indeed tantalizing [7,63,64].

So how is SuperSTEM 3 performing? The early observation of phonon peaks in BN polymorphs [65], whose vibrational response

varies due to different bonding strength in the hexagonal and cubic systems (Fig. 11a), have recently been extended to momentum-resolved spectroscopy. These experiments are here used to access the phonon dispersion characteristics and thus to provide a precise assignment of the modes and a better understanding of their origin [66]. The resulting dispersion curves are in many ways reminiscent of neutron triple axis spectroscopy data – with the important difference that the probe is nm-sized rather than mm-sized (admittedly, the energy and momentum resolutions in the conditions used for the STEM experiments are poorer than in inelastic neutron scattering) [67]. Advanced low loss EELS in real and momentum spaces promises to provide access to the electronic density of states of individual nano-objects: see Fig. 11b-c where this approach is demonstrated on single-wall carbon nanotubes, revealing the dispersion characteristics of van Hove singularities peaks and various plasmon modes [68]. The parallels and increasing overlap between the capabilities of these new instruments and of those of larger-scale facilities are striking. Although there are still obvious limitations of the STEM in generating these types of data which should not be overlooked, one could (mischievously) argue that a synchrotron, a neutron source and a Raman spectrometer are now all “in the microscope”.

Of great interest is the effect that such intense monochromatization has on the probe size. Resolution tests on a combined test specimen (Au particles dispersed on a carbon support) show that far from harming resolution, monochromating the beam to 14meV (full-width at half-maximum of the EELS zero loss peak in vacuum) improves the information transfer. Fig. 12 shows two images taken consecutively, without (Fig. 12, left) and with (Fig. 12, right – recorded with a much longer pixel dwell time to compensate for the reduced, *ca.* 20 times, beam current) the monochromating slit. The Fourier transforms of the images, inset, demonstrate sub-Å information transfer in both cases. Of course, this is not unexpected: as chromatic effects are expected to dominate at lower acceleration voltages [49], reducing the beam energy width should improve resolution. It is however exciting to see it in practice. At 60 kV, the improvement is not expected to be dramatic, but further exploration at lower voltages should theoretically lead to sub-Å, sub-100meV probes at 40 kV [69].

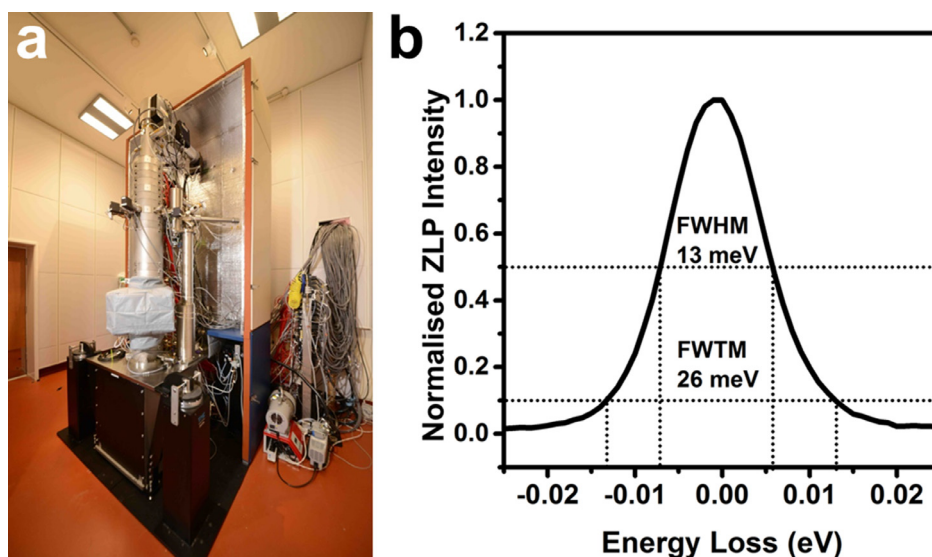


Fig. 10. a) The SuperSTEM 3 microscope, a Nion UltraSTEM100MC 'HERMES', at the SuperSTEM Facility. b) Typical EELS performance of the instrument: 60 kV acceleration voltage, 31mrad convergence angle, 36mrad EELS collection angle, 1meV/channel dispersion, a probe current of ~5–10pA and no data binning. The probe size in these conditions is estimated to be 1.0 Å. The normalised zero-loss peak (ZLP) in vacuum demonstrates a 13meV full-width at half-maximum (FWHM), 26meV full-width at tenth-maximum (FWTM) for a 100 ms spectral acquisition. (Test data courtesy of Dr Fredrik Hage, SuperSTEM).

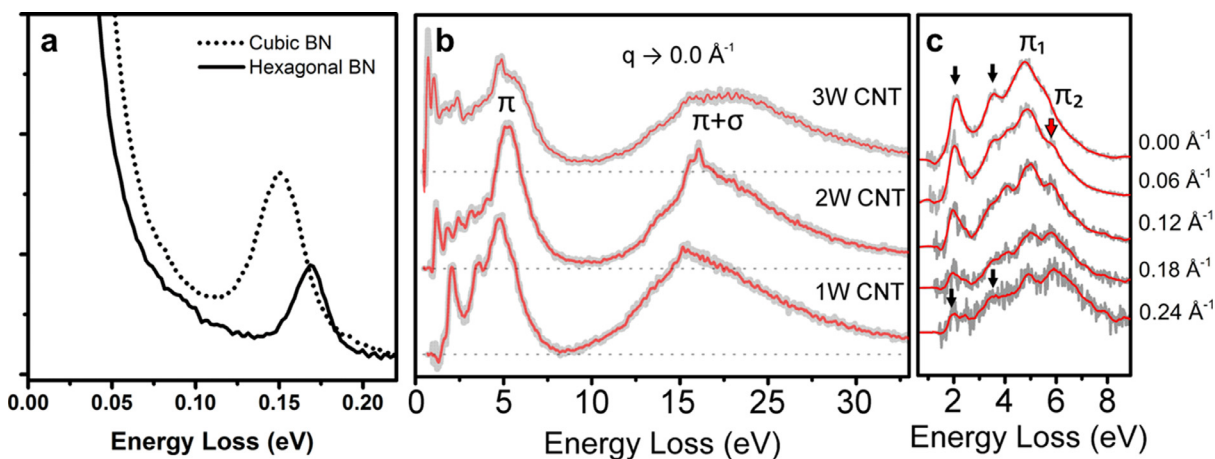


Fig. 11. a) Difference in phonon response for cubic and hexagonal BN [65]. b) Low loss spectroscopy of individual carbon nanotubes in real and momentum spaces, providing insights into the nano-objects' electronic structure. In particular, sharp peaks at energy losses below ~ 5 eV are attributed to π - π^* interband transitions between van Hove singularities in the CNTs' valence and conduction band densities of states [68]. All spectra were acquired at 60 kV on SuperSTEM 3 with an estimated ZLP FWHM of below 20 meV.

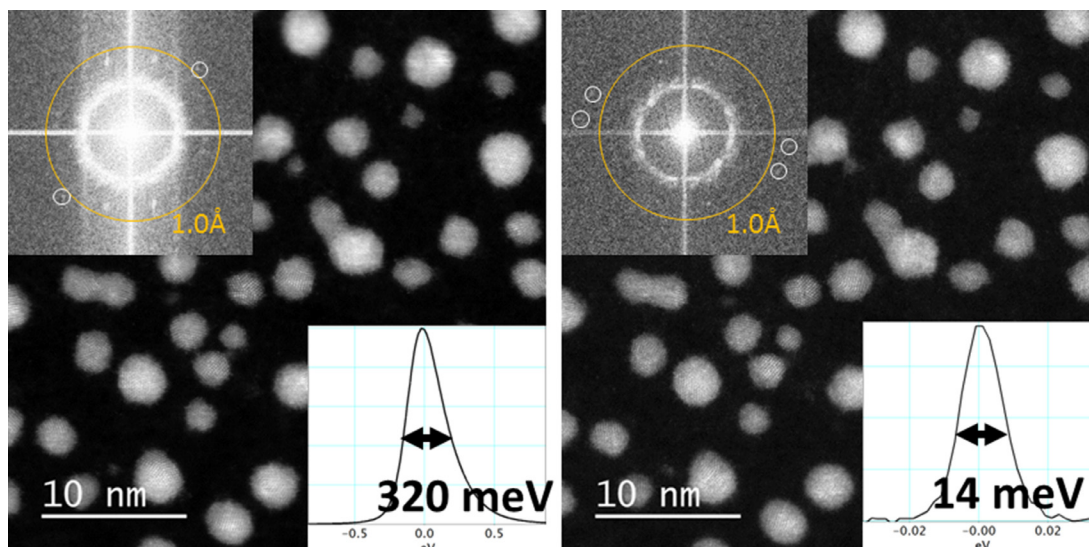


Fig. 12. HAADF images of Au nano-particles dispersed on an amorphous carbon support, taken consecutively, at 60 kV acceleration voltage on the SuperSTEM 3 microscope. Left: the monochromator slit is not inserted resulting in a beam energy width of 320 meV (normalised ZLP recorded in vacuum before the image) and a probe current of approximately 120 pA. Right: the monochromator slit is inserted, resulting in a beam energy width of 14 meV (normalised ZLP acquired in vacuum after the image) and a beam current of approximately 6 pA. The Fourier transforms (inset) demonstrate information transfer beyond 1 Å in both cases. A slight improvement is observed after monochromation.

Finally, turning back to applications highlighted in “A synchrotron in a Microscope”, it is clear that the new generation of monochromators has made the observation of low loss features such as excitons and band gaps in the electron microscope far easier. Tantalizing observations of local (nm-length scale) 20 meV band gap fluctuations correlated with chemical variations in semiconducting photovoltaic thin films have recently been reported [70]. These unique experiments pave the way to band gap (and gap state) mapping at sub-nm resolution. Furthermore, a number of groups have been studying excitonic peaks in single- and multi-layer MoS₂ flakes [71,72]. Importantly, in order to compare directly experimental data to computational results, higher levels of theory than ‘simple’ DFT approaches, which make use of many-body calculations, are now necessary [71]: Fig. 13. It is becoming apparent that the experimental data produced by these new instruments is challenging the state-of-the-art in theoretical calculations for EELS, promising exciting times ahead.

6. Conclusion

It has been nearly twenty years since the 1997 Electron Microscopy and Analysis Group Conference. Two of its seminal lectures are widely considered to mark the start of the aberration-corrected STEM era in the United Kingdom as they provided the impetus for the establishment of its National Facility for STEM, the SuperSTEM Laboratory. This non-exhaustive scan through three generations of SuperSTEM instruments was aimed at illustrating a shared history and at recognizing from a rather personal perspective the impact that aberration correction, and Ondrej Krivanek's work among other pioneers of the field, has had on the microscopy community. Re-reading through the entire conference proceedings volume, which includes the two papers that provided the premise for this manuscript but also many other important papers, is a humbling experience because of the sheer number of visionary contributions that can be found therein. It is an honor to have witnessed the advent of a new era of electron microscopy, and

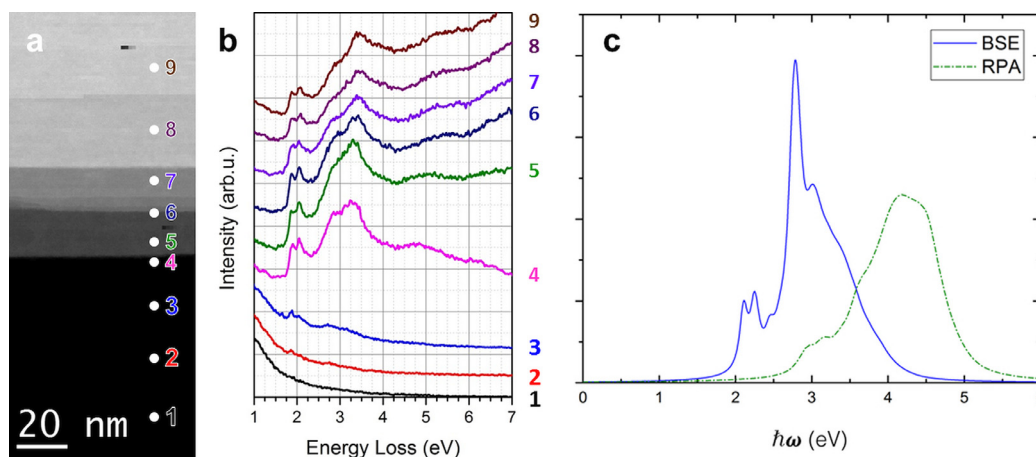


Fig. 13. Position-resolved EELS spectra at the stepped edge of a MoS₂ nano-flake, recorded at 20meV energy resolution on the SuperSTEM 3 microscope. The excitonic A and B peaks are clearly resolved, and the assignment of their excitonic origin is confirmed through *ab initio* calculations. Solving the Bethe-Salpether equation includes the effects of electron-hole coupling and gives rise to the two peaks at 2.1 eV, whereas the more simple random phase approximation (RPA) calculations do not. Adapted with permission from Nerl et al. [71].

perhaps at times played a minor part in it. Without a doubt, Ondrej Krivanek's "Aberration correction in the STEM" has made Mick Brown's "Synchrotron in a Microscope" a reality.

Acknowledgements

The author is truly indebted to Ondrej Krivanek for nearly two decades of shared history with the SuperSTEM Laboratory and around the world – and looks forward to more record-breaking instrumentation developments for the next generation of microscopes he is no doubt already planning. Of course, all the colleagues who contributed to the results discussed in this work are gratefully acknowledged, as well as SuperSTEM crews past – and importantly present (Drs. Patricia Abellan, Iain Godfrey, Fredrik Hage, David Hernandez-Maldonado, Demie Kepaptsoglou and Dorothea Mücke-Herzberg). Finally, Profs. Andrew Bleloch, Mick Brown and Archie Howie provided invaluable mentoring and inspiration. The SuperSTEM Laboratory is the U.K. National Facility for Aberration-Corrected STEM, supported by the Engineering and Physical Sciences Research Council (EPSRC).

References

- [1] L.M. Brown, A Synchrotron in a Microscope, in: J.M. Rodenburg (Ed.), *Electron Microscopy and Analysis 1997*, Institute of Physics Conference Series 153, IOP Publishing, London, 1997, pp. 17–22.
- [2] M. Haider, G. Braunshausen, E. Schwan, Correction of the spherical aberration of a 200kV TEM by means of a hexapole corrector, *Optik* 99 (1995) 167–179.
- [3] P.W. Hawkes, The correction of electron lens aberrations, *Ultramicroscopy* 156 (2015) A1–A64.
- [4] J. Zach, M. Haider, Correction of spherical and chromatic aberration in a low voltage SEM, *Optik* 93 (1995) 112–118.
- [5] O.L. Krivanek, Private communication, 2015.
- [6] O.L. Krivanek, N. Dellby, A.J. Spence, et al., Aberration correction in the STEM, in: J.M. Rodenburg (Ed.), *Electron Microscopy and Analysis 1997*, Institute of Physics Conference Series 153, IOP Publishing, London, 1997, pp. 17–22.
- [7] O.L. Krivanek, T.C. Lovejoy, N. Dellby, Vibrational spectroscopy in the electron microscope, *Nature* 514 (2014) 209–212.
- [8] P.W. Hawkes, Aberration correction past and present, *Phil. Trans. R. Soc. A* 367 (2009) 3637–3664.
- [9] O. Scherzer, Sphärische und chromatische Korrektur von Elektronenlinsen, *Optik* 8 (1947) 311–317.
- [10] O.L. Krivanek, N. Dellby, A.J. Spence, et al., On-line aberration measurement and correction in STEM, *Microscopy and Microanalysis* 3, in: S3: Proceedings of the 55th MSA Meeting, 1997, pp. 1171–1172.
- [11] O.L. Krivanek, N. Dellby, A.R. Lupini, Towards sub-Å electron beams, *Ultramicroscopy* 78 (1999) 1–11.
- [12] O.L. Krivanek, Method for determining the coefficient of spherical aberration from a single electron micrograph, *Optik* 45 (1975) 97–101.
- [13] O.L. Krivanek, S. Isoda, K. Kobayashi, Accurate stigmating of a high voltage electron microscope, *J. Microsc.* 111 (1977) 279–282.
- [14] O.L. Krivanek, G.Y. Fan, Application of slow-scan CCD cameras to on-line microscope control, *Scann. Microsc. Suppl.* 6 (1994) 105–114.
- [15] A. Bleloch, Q.M. Ramasse, Lens aberrations: diagnosis and correction, in: R. Brydson (Ed.), *Aberration-Corrected Analytical Transmission Electron Microscopy*, Wiley, London, 2011.
- [16] A.R. Lupini, Aberration Correction in STEM, PhD Thesis, Cambridge University, Cambridge, U.K., 2001.
- [17] Q.M. Ramasse, Diagnosis of Aberrations in Scanning Transmission Electron Microscopy, PhD Thesis, Cambridge University, Cambridge, U.K., 2005.
- [18] S. Uno, K. Honda, N. Nakamura, M. Matsuya, J. Zach, Aberration correction and its automatic control in scanning electron microscopes, *Optik* 116 (2005) 438–448.
- [19] A.R. Lupini, The Electron Ronchigram, in: S.J. Pennycook, P.D. Nellist (Eds.), *Scanning Transmission Electron Microscopy Imaging and Analysis*, Springer, New York, 2011.
- [20] N. Dellby, O.L. Krivanek, P.D. Nellist, et al., Progress in aberration-corrected scanning transmission electron microscopy, *J. Electron Microsc.* 50 (2001) 177–185.
- [21] A.R. Lupini, P. Wang, P.D. Nellist, et al., Aberration measurement using the Ronchigram contrast transfer function, *Ultramicroscopy* 110 (2010) 891–898.
- [22] O.L. Krivanek, N. Dellby, A.R. Lupini, Patent: Autoadjusting charged particle probe-forming apparatus, US6552340B1 (2003)
- [23] Q.M. Ramasse, A.L. Bleloch, Diagnosis of aberrations from crystalline samples in scanning transmission electron microscopy, *Ultramicroscopy* 106 (2005) 37–56.
- [24] J. Barthel, A. Thust, Aberration measurement in HRTEM: implementation and diagnostic use of numerical procedures for the highly precise recognition of diffraction patterns, *Ultramicroscopy* 111 (2010) 27–46.
- [25] H. Sawada, T. Sannomiya, F. Hosokawa, Measurement method of aberration from Ronchigram by autocorrelation function, *Ultramicroscopy* 108 (2008) 1467–1475.
- [26] J. Barthel, A. Thust, On the stability of high-resolution transmission electron microscopes, *Ultramicroscopy* 134 (2013) 6–17.
- [27] M.W. Tate, P. Purohit, D. Chamberlain, High dynamic range pixel array detector for scanning transmission electron microscopy, *Microsc. Microanal.* 22 (2016) 237–249.
- [28] H. Yang, T.J. Pennycook, P.D. Nellist, Efficient phase contrast imaging in STEM using a pixelated detector. Part II: Optimisation of imaging conditions, *Ultramicroscopy* 151 (2015) 232–239.
- [29] A.R. Lupini, M. Chi, S. Jesse, Rapid aberration measurement with pixelated detectors, *Journal of Microscopy* 263 (2016) 43–50.
- [30] S. Zhao, Y. Li, E. Stavitski, et al., Operando characterization of catalysts through the use of a portable microreactor, *ChemCatChem* 7 (2015) 3683–3691.
- [31] P.E. Batson, N. Dellby, O.L. Krivanek, Sub-angstrom resolution using aberration corrected electron optics, *Nature* 418 (2002) 617–620.
- [32] P.D. Nellist, M.F. Chisholm, N. Dellby, et al., Direct sub-angstrom imaging of a crystal lattice, *Science* 305 (2004) 1741.
- [33] R. Erni, P. Tiemeijer, M. van der Stam, et al., A new era of analysis with spherical-aberration-corrected STEM – atomic and electronic information approaching the single atom level, *Microsc. Microanal.* 12 (S2) (2006) 1372–1373.
- [34] H. Sawada, T. Tomita, M. Naruse, Experimental evaluation of a spherical aberration-corrected TEM and STEM, *Microscopy* 54 (2005) 119–121.
- [35] I. Arlsan, A. Bleloch, E.A. Stach, N.D. Browning, Atomic and electronic structure of mixed and partial dislocations in GaN, *Phys. Rev. Lett.* 94 (2005) 025504.

- [36] A.L. Bleloch, Scanning transmission electron microscopy and electron energy loss spectroscopy: mapping materials atom by atom, in: P.W. Hawkes (Ed.), *Advances in Imaging and Electron Physics*, vol. 153, Elsevier, 2008, pp. 195–223.
- [37] U. Falke, A. Bleloch, M. Falke, et al., Atomic structure of a (2x1) reconstructed NiSi₂/Si(001) interface, *Phys. Rev. Lett.* 92 (2004) 116103.
- [38] P. Agrawal, M.D. Rossell, C. Hébert, et al., Dislocation modelling: calculating EELS spectra for edge dislocation in bismuth ferrite, in: *Proceedings of the 16th European Microscopy Congress*, Lyon, 2016, doi:10.1002/9783527808465.EMC2016.5913.
- [39] M. Arredondo, Q.M. Ramasse, M. Weyland, et al., Direct evidence for cation non-stoichiometry and Cottrell atmospheres around dislocation cores in functional oxide interfaces, *Adv. Mater.* 22 (2009) 2430–2434.
- [40] C. Kisielowski, B. Freitag, M. Bischoff, et al., Detection of single atoms and buried defects in three dimensions by aberration-corrected microscope with 0.5Å information limit, *Microsc. Microanal.* 14 (2008) 469–477.
- [41] G. Yang, Q. Ramasse, R.F. Klie, Direct measurement of charge transfer in thermoelectric Ca₃Co₄O₉, *Phys. Rev. B* 78 (2008) 153109.
- [42] P. Yu, W. Luo, J.X. Zhang, Interface control of bulk ferroelectric polarization, *Proc. Natl. Acad. Sci., USA* 109 (2011) 9710–9715.
- [43] M. Bosman, V.J. Keast, J.L. Garcia-Munoz, Two-dimensional mapping of chemical information at atomic resolution, *Phys. Rev. Lett.* 99 (2007) 086102.
- [44] K. Kimoto, T. Asaka, T. Nagai, Element-selective imaging of atomic columns in a crystal using STEM and EELS, *Nature* 450 (2007) 702–704.
- [45] E.J. Monkman, C. Adamo, J.A. Mundy, Quantum many-body interactions in digital oxide superlattices, *Nat. Mater.* 11 (2012) 855–859.
- [46] M.H. Gass, U. Bangert, A.L. Bleloch, et al., Free-standing graphene at atomic resolution, *Nat. Nanotechnol.* 3 (2008) 676–681.
- [47] O.L. Krivanek, Private communication, 2009.
- [48] O.L. Krivanek, N. Dellby, M.F. Murfitt, Gentle STEM: ADF imaging and EELS at low primary energies, *Ultramicroscopy* 110 (2010) 935–945 2010a.
- [49] O.L. Krivanek, W. Zhou, M.F. Chisholm, Gentle STEM of Single Atoms: low keV imaging and analysis at ultimate detection limits, in: D.C. Bell, N. Erdmann (Eds.), *Low Voltage Electron Microscopy: Principles and Applications*, Wiley, London, 2013.
- [50] R.F. Egerton, Control of radiation damage in the TEM, *Ultramicroscopy* 127 (2013) 100–108.
- [51] O.L. Krivanek, M.F. Murfitt, V. Nicolosi, Atom-by-atom structural and chemical analysis by annular dark field electron microscopy, *Nature* 464 (2010) 571–574 2010b.
- [52] L.P. Hansen, Q.M. Ramasse, C. Kisielowski, Atomic-scale edge structures on industrial-style MoS₂ nanocatalysts, *Angew. Chem. Int. Ed.* 50 (2011) 10153–10156.
- [53] R. Zan, Q.M. Ramasse, U. Bangert, K.S. Novoselov, Graphene reknits its holes, *Nano Lett.* 12 (2012) 3936–3940.
- [54] K. Suenaga, Y. Sato, Z. Liu, Visualizing and identifying single atoms using electron energy-loss spectroscopy with low accelerating voltage, *Nat. Chem.* 1 (2009) 415–418.
- [55] U. Bangert, W. Pierce, D.M. Kepaptsoglou, Ion implantation of graphene: towards IC compatible technologies, *Nano Lett.* 13 (2013) 4902–4907.
- [56] T.C. Lovejoy, Q.M. Ramasse, M. Falke, Single atom identification by energy dispersive X-ray spectroscopy, *Appl. Phys. Lett.* 100 (2012) 154101.
- [57] K. Suenaga, T. Okazaki, E. Okunishi, et al., Detection of photons emitted from single erbium atoms in energy-dispersive X-ray spectroscopy, *Nat. Photon.* 6 (2012) 545–548 2012b.
- [58] K. Suenaga, M. Koshino, Atom-by-atom spectroscopy at graphene edge, *Nature* 468 (2010) 1088–1090.
- [59] K. Suenaga, H. Kobayashi, M. Koshino, Core-level spectroscopy of point defects in single layer h-BN, *Phys. Rev. Lett.* 108 (2012) 075501 2012a.
- [60] Q.M. Ramasse, C.R. Seabourne, D.M. Kepaptsoglou, Probing the bonding and electronic structure of single atom dopants in graphene with electron energy loss spectroscopy, *Nano Lett.* 13 (2013) 4989–4995.
- [61] W. Zhou, M.D. Kepatenakis, M.P. Prange, Direct determination of the chemical bonding of individual impurities in graphene, *Phys. Rev. Lett.* 109 (2012) 206803.
- [62] D. Kepaptsoglou, T.P. Hardcastle, C.R. Seabourne, Electronic structure modification of ion-implanted graphene: the spectroscopic signatures of p- and n-type doping, *ACS Nano* 9 (2015) 11398–11407.
- [63] T. Miyata, M. Fukuyama, A. Hibara, Measurement of vibrational spectrum of liquid using monochromated scanning transmission electron microscopy-energy loss spectroscopy, *Microscopy* 63 (2014) 377–382.
- [64] P. Rez, T. Aoki, K. March, Damage-free vibrational spectroscopy of biological materials in the electron microscope, *Nat. Commun.* 7 (2016) 10945.
- [65] R. Nicholls, F.S. Hage, K. Refson, Vibrational phonon spectroscopy of boron nitride polymorphs: a comparison between theory and experiment, *Microsc. Microanal.* 21 (S3) (2015) 1469–1470.
- [66] Q.M. Ramasse, F.S. Hage, D.M. Kepaptsoglou, Recent applications of sub-20meV monochromated STEM-EELS: from phonon to core losses in real and momentum spaces, *Microsc. Microanal.* 22 (S3) (2016) 964–965.
- [67] F.S. Hage, R. Nicholls, K. Refson et al. Momentum-resolved vibrational spectroscopy of individual nano-objects in the STEM, in preparation, 2016.
- [68] F.S. Hage, Q.M. Ramasse, The low loss spectrum of individual carbon nanotubes revisited at high energy resolution in real and momentum space, *Microsc. Microanal.* 22 (S3) (2016) 966–967 2016a.
- [69] T.C. Lovejoy, Private communication, 2016.
- [70] D. Keller, S. Buecheler, P. Reinhard, Band gap widening at random CIGS grain boundary detected by valence electron energy loss spectroscopy, *Appl. Phys. Lett.* 109 (2016) 153103.
- [71] H. Nerl, K. Winther, F.S. Hage, Probing the local nature of excitons and plasmons in few-layer MoS₂, *NPJ 2D Materials and Applications*, 2016, in press.
- [72] L.H.G. Tizei, Y.-C. Lin, M. Mukai, Exciton mapping at sub-wavelength scales in two-dimensional materials, *Phys. Rev. Lett.* 114 (2015) 107601.